ELSEVIER

Nuclear Instruments and Methods in Physics Research A 445 (2000) 247–252

NUCLEAR INSTRUMENTS & METHODS IN PHYSICS RESEARCH Section A

www.elsevier.nl/locate/nima

Super-radiance in a prebunched beam free electron maser

M. Arbel[a,*], A.L. Eichenbaum[a], Y. Pinhasi[b], Y. Lurie[b], M. Tecimer[a], A. Abramovich[a], H. Kleinman[a], I.M. Yakover[a], A. Gover[a]

[a]*Department of Physical Electronics, Tel-Aviv University, P.O.B. 39040, Ramat Aviv, Tel Aviv 69978, Israel*
[b]*Department of Electrical and Electronics Engineering, The College of Judea and Samaria, Ariel, Israel*

Abstract

It is well known that electrons passing through a magnetic undulator emit partially coherent radiation: "Undulator Synchrotron Radiation". Radiation from electrons, entering the undulator at random, adds incoherently. If the electron beam is periodically modulated (bunched) to pulses shorter than the radiation wavelength, electrons radiate in phase with each other, resulting in super-radiant emission at the bunching frequency. Introduction of a signal at the input of the prebunched beam FEL, results in stimulated super-radiant emission. The interaction between the electromagnetic wave and a synchronous modulated e-beam results in amplification of the signal wave in addition to the spontaneous super-radiant emission. We demonstrated and measured the super-radiant emission in a wide band of frequencies from 3.15 to 5.5 GHz using the mini-FEM of Tel-Aviv University, wherein pre-bunching at the radiation frequency is accomplished with the aid of a traveling-wave prebuncher. The measured upper synchronous frequency is centered about 4.5 GHz and the lower synchronous frequency is just above cutoff (near 3.153 GHz). Analytical models, computer simulations and experimental results of a pre-bunched free-electron laser operation are presented and compared. The power levels that can be achieved are discussed. The measured results agree well with results predicted theoretically and obtained by a 3D simulation code.

Keywords: Free electron maser; Super radiance; Prebunched; Modulation

1. Introduction

Electron beam bunching over an extent smaller than the radiation wavelength leads to emission of partially coherent undulator synchrotron radiation (several orders of magnitude greater than the non-coherent radiation obtained from an unmodulated e-beam) [1].

The radiation obtained from a periodically pre-modulated e-beam traversing a waveguiding structure, located in a magnetic undulator of the type employed in free electron lasers/masers has been the subject of several recent investigations [2–6]. The analytical treatment in Ref. [2] is based on a one-dimensional FEL model which takes into account space charge, current density and velocity modulation and characterizes the radiated power in the low- and high-gain regimes for low and high space charge density e-beams.

The analysis in Ref. [3] is one-dimensional and does not include velocity modulation. Measurements

* Corresponding author. Tel.: +972-3-640-8148; fax: +972-3-642-3508.
E-mail address: arbel@eng.tau.ac.il (M. Arbel).

0168-9002/00/$ - see front matter
PII: S0168-9002(00)00077-2

described in Ref. [4] were made at a very low e-beam current and were compared to predictions, made on the basis of Ref. [3].

Super-radiant spontaneous emission in waveguide-type FELs at the lower synchronous frequency (near to cutoff) is predicted to be stronger than the prebunched beam radiation at the higher synchronous frequency [2,5]. Based on a three-dimensional FEL model [7] we calculated gain, oscillation buildup and super-radiant emission over the whole frequency range of interest in the linear and nonlinear regimes of operation taking into account space charge, current density and velocity modulation and the phase between them.

We compared calculated results of super-radiant emission based on Refs. [2,6] with measurements of super-radiant emission from a compact waveguide-type, Free Electron Maser which utilizes a very broad band traveling wave-type prebuncher [8]. The prebuncher allows controlled e-beam prebunching at any radiation frequency from waveguide cutoff to frequencies well above the higher frequency synchronous band.

The simulation results obtained by the FEL 3D code [7] were compared with measured values of super-radiant emission obtained from 55 to 70 kV, 0.1 to 0.7 A e-beam modulated at the fundamental frequency (with a modulation parameter varying from 0 to 0.3) throughout the frequency range of interest (from cutoff at 3.15–5.5 GHz). Excellent correlation between the measurement and simulation results indicates the validity of the simulations.

2. Super-radiant emission from prebunched beams

A prebunched beam with a sinusoidal modulated current at a frequency f_o:

$$\mathrm{i}(t) = I_o[1 + m\cos(2\pi f_o t)] \tag{1}$$

(where I_o is the average (DC) current and m is the modulation depth) emits coherent radiation (super-radiance) at the bunching frequency while passing through a wiggler. The power at the exit of the interaction region (the wiggler of length L_w) is given by [6]

$$P_{sr}(L_w) = P_B \cdot \sin c^2[\tfrac{1}{2}\theta(\omega_o)L_w] \tag{2}$$

where the prebunching power parameter is

$$P_B = \frac{m^2}{32} I_o^2 L_w^2 \left(\frac{a_w}{\gamma_o \beta_{oz}}\right)^2 \frac{Z_{mode}}{A_{em}} \tag{3}$$

where Z_{mode}, A_{em} are the impedance and effective area of the excited waveguide mode, respectively, and $\theta(\omega_o) = \omega_o/v_{zo} - (k_z(\omega_o) + k_w)$ is the detuning parameter. The expression given in Eq. (2) for the super-radiance power does not take into account space charge effects or amplification. Observe that the radiated power is proportional to the square of the AC component $(mI_o)^2$ of the modulated current given in Eq. (1).

Modulation of e-beams can be expressed in terms of both current density and velocity modulation [2]. Based on the work of Ref. [6] we developed a computer code [7] for a sinusoidally modulated e-beam, which takes into account space charge, sinusoidal current density and velocity modulation and the phase between them.

3. Experimental setup and measurements

The compact prebunched beam FEM developed at Tel-Aviv University is shown in Fig. 1. Its operation as an oscillator which permits mode selection and single-frequency operation via prebunching was described [9] as well as efficiency enhancement possibility by selection of an appropriate eigenfrequency [10]. Applications as a frequency agile oscillator (on a pulse-to-pulse basis) were also described [11].

The premodulated e-beam is derived from a traveling-wave-type prebuncher [8], utilizing a Pierce gun. The gridded gun permits convenient current control and the whole gun is held negative with respect to the grounded wiggler. The gun bias with respect to the wiggler determines the beam energy. The e-beam modulation frequency (continuously adjustable over more than an octave bandwidth) is simply the input frequency to the traveling wave prebuncher. At the fundamental frequency the prebunching modulation level $0 \le m \le 1$ at the prebuncher output is proportional to the square root of the prebuncher RF input power ($P_{\mathrm{r.f.\ in}}$) in the

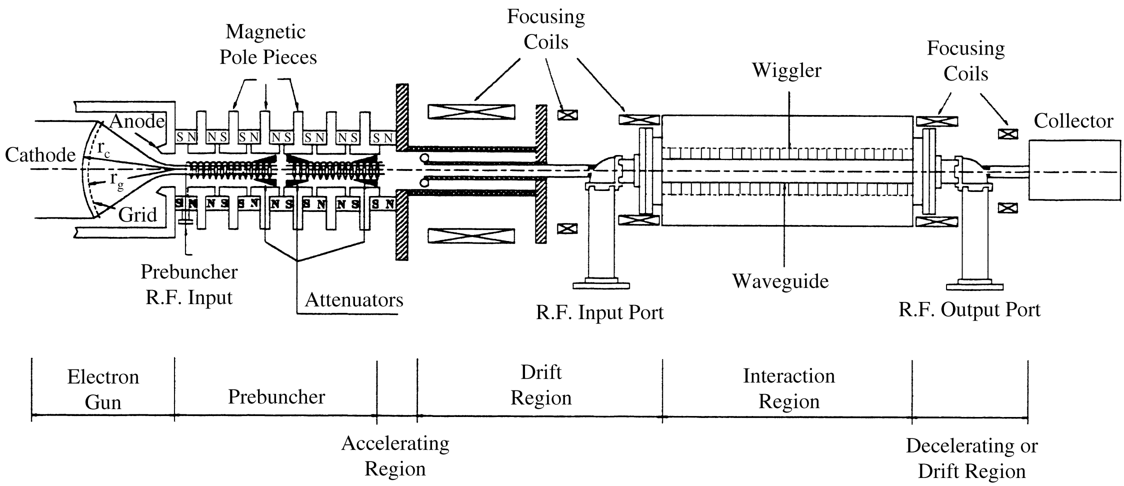

Fig. 1. Schematic illustration of Traveling Wave (TW) prebunched Free Electron Maser.

linear region of the prebuncher [8]. Consequently, the super-radiant power $P_{sr}(L_w)$ obtained at the FEL output (2) is proportional to the bunching power $P_{RF.\ in}$ introduced to the prebuncher.

The premodulated e-beam derived from the prebuncher traverses a rectangular WR-187 waveguide located in the "wiggler" section. At 70 keV beam energy the two predicted synchronous frequencies in the TE10 mode are: just above cutoff (near 3.153 GHz) and at about 4.9 GHz (see Fig. 2). The setup for measuring prebunched beam radiation is shown in Fig. 3. The input and output RF ports of the FEM are terminated in matched loads. The prebunching frequency and e-beam prebunching level are simply set by the signal generator frequency and its internal attenuator, respectively. The e-beam energy and current are determined by the e-gun voltages as described above.

The flexibility of FEM operating parameters is indicated by Table 1.

Maximum modulation ($m \approx 1$) at the prebuncher output is obtained for an RF input power $P_{RF\ opt} \approx 2$ W to the prebuncher which is about 10 dB lower than the input which saturates the prebuncher. For RF input power below 2 W m^2 is proportional to $P_{RF\ in}/P_{RF\ opt}$. We, thus, have the ability to control the prebunching level and frequency via the RF input power and frequency

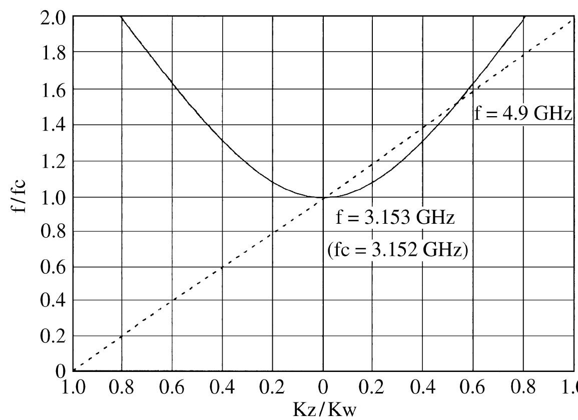

Fig. 2. The waveguide dispersion curve and the electron beam line.

to the prebuncher. The RF input power to the prebuncher which produces maximum prebunching in the beam is a function of frequency, because of the nonconstant frequency response of the prebuncher [8].

Measurement of radiated power versus prebuncher RF input power (Fig. 4) indicates that the radiated power is indeed proportional to the RF input power $P_{RF\ in}$. This allows estimation of the modulation parameter at each RF input level.

For $m \approx 1$ at the exit of the prebuncher it was estimated in Ref. [8] that at the entrance to the

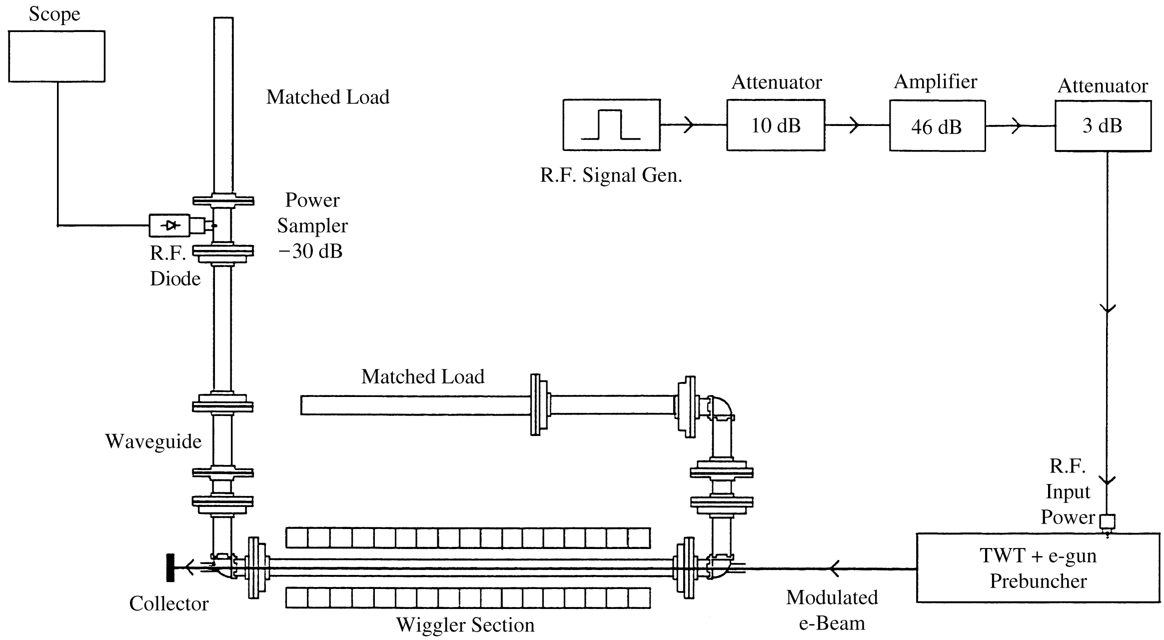

Fig. 3. Schematic of experimental setup for measuring the super-radiance emission.

Table 1
Parameters of the mini FEM

Electron accelerator	Pierce gun + electrostatic accelerator
Electron beam energy	50–70 keV
Electron beam current	0.1–0.7 Amp
Electron beam prebuncher	Traveling-wave type
Prebuncher frequency band	3 GHz $\leq f_m \leq$ 12 GHz
Prebuncher input power	$O \leq P_{Pb} \leq 3$ W
Prebuncher current modulation depth	$O \leq m_j \leq 1$
Wiggler type	Hallbach magnetostatic
Magnetic induction	300 Gauss
Length of period	4.44 cm
Number of periods	$N_W = 17$
Interaction length	$L_W = 85$ cm
Waveguide type	WR − 187
Rectangular waveguide	2.215 cm × 4.755 cm
Mode	TE_{10}
TE_{10} cutoff frequency	$f_c = 3.153$ GHz

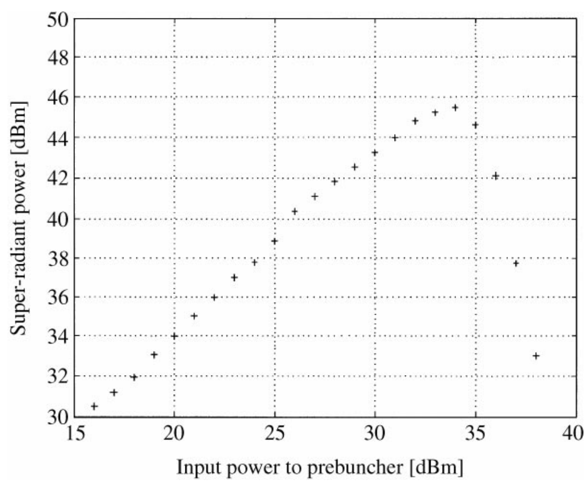

Fig. 4. Super-radiance power vs. RF input power to TW prebuncher.

"wiggler" (for a drift distance of 0.5 m between them) the maximum value of the modulation is $m \approx 0.35$.

The super-radiant power was measured as a function of the electron beam DC current I_o at a frequency of 4.42 GHz. Comparison of measured radiation power with theoretical calculations and simulations is shown in Fig. 5.

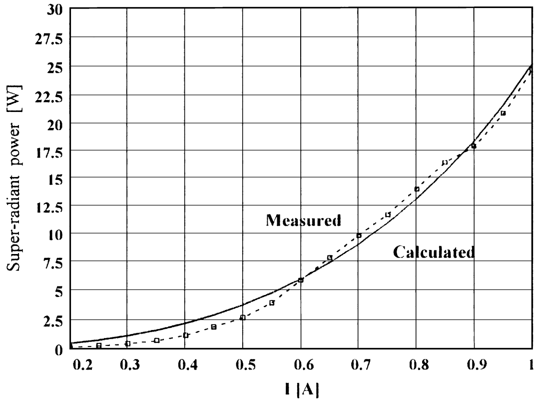

Fig. 5. Super-radiance power vs. e-beam current.

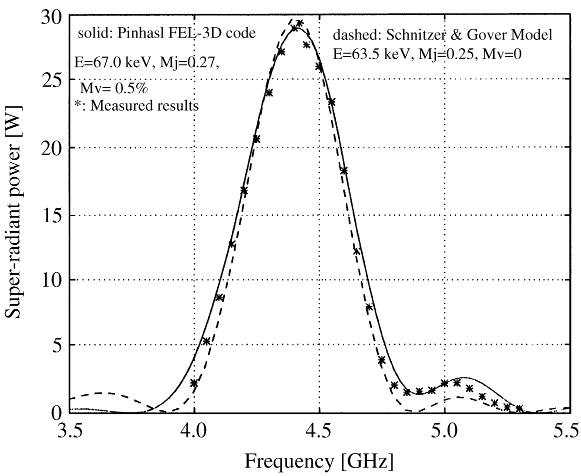

Fig. 6. Comparison of measured super-radiance power vs. frequency. with simulations and calculations.

The super-radiant power in the vicinity of the upper frequency synchronism was measured for a set of conditions of our experiment as per Table 1 with $I = 0.7$ A and maximal beam prebunching. We calculated super-radiant power based on Ref. [2] and simulations were made according to Ref. [7]. As shown in Fig. 6 good agreement of measured data was obtained with calculations based on Ref. [2] if a beam energy 63.5 keV was used in the calculations (instead of the 70 keV experimentally employed) and a current modulation parameter $m_j = 0.25$. Simulations based on Ref. [7]

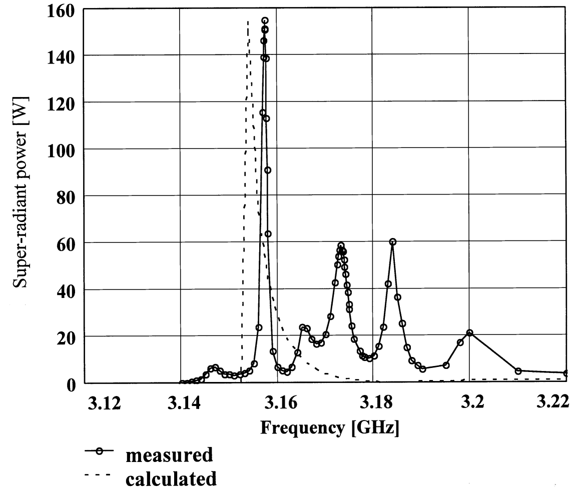

Fig. 7. Super-radiance power vs. frequency near waveguide cutoff.

provide good agreement for a beam energy corresponding to 67.0 keV, a current modulation parameter $m_j = 0.27$and a velocity modulation parameter $m_v = 0.5\%$. These current and velocity modulation parameters are close to those estimated in Ref. [8] for our experimental conditions.

4. Super-radiance near waveguide cutoff

In an experiment carried out recently we measured super-radiance power near waveguide cutoff. For our FEM parameters the lower synchronous frequency is slightly above waveguide cutoff (near 3.153 GHz). According to analytical models [2,5,12] and FEL 3D simulations the expected super-radiance power near cutoff is about 5 times larger than that of the higher synchronous frequency and the predicted spectral width of the radiated power near cutoff is much smaller. In a series of wide band measurements we verified the existence of strong super-radiance and the spectral characteristics of the radiation near cutoff. Based on Ref. [2] we carried out calculations of expected radiation near cutoff for our experimental conditions. The calculated and measured radiation near cutoff is shown in Fig. 7. The observed radiation near cutoff corresponds qualitatively to these simulations. We will continue these experiments for other e-beam energies and for other operating conditions.

References

[1] H. Motz, J. App. Phys. 22 (1951) 527.
[2] I. Schnitzer, A. Gover, Nucl. Instr. and Meth. A 237 (1985) 124.
[3] A. Doria et al, IEEE J. Quantum Electron. QE-29 (1993) 1428.
[4] S. Mayhew et al., Nucl. Instr. and Meth. A 393 (1997) 356.
[5] I.M. Yakover, Nucl. Instr. and Meth. A 393 (1997) 316.
[6] Y. Pinhasi, Ph.D. Thesis, Tel-Aviv University, 1995.
[7] Y. Pinhasi, V. Shterngartz, A. Gover, Phys. Rev. E 54 (1996) 6774.
[8] A. Eichenbaum, IEEE Trans. Plasma Sci. 27(2) 568.
[9] M. Cohen et al., Phys. Rev. Lett. 74 (1995) 3812.
[10] A. Abramovich et al., Nucl. Instr. and Meth., to be published.
[11] A. Eichenbaum et al., Proceedings of the 18th conference on IEEE in Israel, Vol. 444, 1995, pp. 1–5.
[12] M. Cohen, Ph.D. Thesis, Tel-Aviv University, 1995.